SOFT ROBOTICS Volume 00, Number 00, 2020 © Mary Ann Liebert, Inc. DOI: 10.1089/soro.2020.0016 SORO-2020-0016-ver9-Sankar_1P
Type: research-article



ORIGINAL ARTICLE

Texture Discrimination with a Soft Biomimetic Finger Using a Flexible Neuromorphic Tactile Sensor Array That Provides Sensory Feedback

AU1 ► Sriramana Sankar,^{1,*} Darshini Balamurugan,^{2,*} Alisa Brown,¹ Keqin Ding,¹ Xingyuan Xu,³ Jin Huat Low,⁴ Chen Hua Yeow,⁴ and Nitish Thakor^{1,4,5}

AU3 ► Abstract

The compliant nature of soft fingers allows for safe and dexterous manipulation of objects by humans in an unstructured environment. A soft prosthetic finger design with tactile sensing capabilities for texture discrimination and subsequent sensory stimulation has the potential to create a more natural experience for an amputee. In this work, a pneumatically actuated soft biomimetic finger is integrated with a textile neuromorphic tactile sensor array for a texture discrimination task. The tactile sensor outputs were converted into neuromorphic spike trains, which emulate the firing pattern of biological mechanoreceptors. Spike-based features from each taxel compressed the information and were then used as inputs for the support vector machine classifier to differentiate the textures. Our soft biomimetic finger with neuromorphic encoding was able to achieve an average overall classification accuracy of 99.57% over 16 independent parameters when tested on 13 standardized textured surfaces. The 16 parameters were the combination of 4 angles of flexion of the soft finger and 4 speeds of palpation. To aid in the perception of more natural objects and their manipulation, subjects were provided with transcutaneous electrical nerve stimulation to convey a subset of four textures with varied textural information. Three able-bodied subjects successfully distinguished two or three textures with the applied stimuli. This work paves the way for a more human-like prosthesis through a soft biomimetic finger with texture discrimination capabilities using neuromorphic techniques that provide sensory feedback; furthermore, texture feedback has the potential to enhance user experience when interacting with their surroundings.

Keywords: soft biomimetic finger, flexible tactile sensor, neuromorphic encoding, supervised learning, sensory feedback

Introduction

Interest in soft robotics has grown over the past couple of decades largely due to their compliant structure that tends to be more biomimetic and suitable for tasks such as delicate object handling and palpation. Currently, soft robots have been adapted to a variety of areas such as locomotion, minimally invasive surgery, and orthoses. ^{1–4} A variety of soft orthoses have been developed for hand, elbow, and ankle

rehabilitation as well as for suction liners, prostheses, and human augmentation systems.^{5–9} Since soft robots have the potential to mimic organisms and interface with human bodies, there is an increased trend toward the development of biomimetic robotic grippers and prostheses.^{8,10–18} While these designs have a great grasping capacity, most soft fingers have limited dexterity and sensing capabilities. A few soft fingers have independent, interphalangeal actuation producing more than one degree of freedom (DOF).^{15,19} However,

AU2▶

¹Department of Biomedical Engineering, Johns Hopkins University, Baltimore, Maryland, USA.

²Laboratory for Computational Sensing and Robotics, Johns Hopkins University, Baltimore, Maryland, USA.

School of Automation Science and Electrical Engineering, Beihang University, Beijing, China.

⁴Department of Biomedical Engineering, National University of Singapore, Singapore, Singapore.

SINAPSE Laboratory, National University of Singapore, Singapore, Singapore

^{*}Both these authors are co-first authors.

2 SANKAR ET AL.

none have incorporated texture sensing and sensory feedback capabilities. This study attempts to address this need.

The compliant nature of soft robots give them an advantage over rigid continuum robots because the soft manipulator allows for a more conforming grasp when manipulating objects of diverse sizes, shapes, and texture. Additionally, most soft robots are underactuated, meaning that the DOF do not necessarily correspond to the number of joints. This allows soft robots to have increased complexity and movement without adding additional components. 20 Soft robots are built using compliant materials such as silicone, polymer, rubber, or combined soft and rigid materials creating endo- or exoskeletons with soft actuators. ^{10,18,21} Due to the prevalence of flexible materials and multiple extruders, many soft robots are three-dimensional (3D)-printed without any need for assembly, further reducing the costs.8 Soft robotic actuators range from pulley systems, pneumatics, to hydraulics.²⁰ Pneumatic actuators are most common because air is lightweight, omnipresent, and inviscid. Given these benefits, this study designed a pneumatically actuated biomimetic finger that is fabricated from silicone and fabric.

When subjects receive static and dynamic sensory cues during tactile sensing, they can understand and dynamically interact with their surroundings. Static cues can be obtained instantaneously, with a few studies incorporating these cues, such as temperature, curvature, and force, into their soft robots. 16,17,22,23 Processing dynamic cues, such as texture, is more complex as it requires spatial and temporal information. Identifying surface texture has been shown to be a desirable capability using tactile sensing and feedback as an aid to surgeons during minimally invasive surgery. 24,25 Additionally, tactile sensing has been shown to help prosthesis users with handling everyday objects. 26,27 This idea of texture recognition was proposed by our group in preliminary studies with soft robots, particularly in prosthetic applications. 28,29 Various tactile sensors made from multiple materials have been used for texture discrimination tasks in previous studies.30-41 Several studies tested their sensor and texture discrimination methods on sets of 2–15 grated textures, ^{30–36} whereas fewer studies used a smaller subset of natural textures. ^{37–41} While these sensors perform fairly well at texture discrimination tasks, they do not use a flexible textile sensor that is easily incorporable into the soft biomimetic finger. Additionally,

most of these sensors do not neuromorphically encode the sensory information for texture discrimination.

Neuromorphic encoding is a method to mimic the response of mechanoreceptors found in human skin that transduce tactile information as neural spike train code. To model biomimetic tactile sensing, encoding, and feedback for our system, it is desirable to understand and model these tactile receptors. This process is inspired by the behavior of neurons in transmitting and processing information. Neuromorphic encoding of the spike train and its subsequent processing is more computationally efficient at encoding spatial and temporal information than standard analog data. ^{33,37,42,43} Additionally, neuromorphic encoding allows for easier integration with neuroprostheses as the biomimetic spiking activity can be delivered directly to the skin or afferent nerves to elicit more natural sensory perception. 44,45 Such tactile feedback, mimicking the skin receptors and sensory nerve's code, has the potential to reduce the learning time required for the brain to adapt to using the neuroprosthesis.⁴³ Neuromorphic encoding and spike-based decoding have been used for texture discrimination tasks in previous studies. ^{30,37,46,47} However, this study combines the benefits of the soft biomimetic finger with the integrated flexible, textile tactile sensor and uses neuromorphic encoding with support vector machine (SVM), while also providing users with sensory feedback.

The goal of this study is to demonstrate the texture discrimination capabilities of a novel soft biomimetic finger that is pneumatically actuated and lays the foundation for a prosthetic finger with palpation and sensory feedback capabilities. The work presented here builds on our preliminary studies, 28,29 where we first presented the prototype design of a soft finger and the use of tactile sensors. Now, in this work, we fully investigate the effects of palpation speed and actuation on texture discrimination using the soft finger and explore the use of sensory feedback (Fig. 1). This article first presents the comprehensive design of the soft biomimetic finger and the textile tactile sensor array. The tactile sensor response is encoded in a biomimetic manner, mimicking the properties of skin tactile receptors. Then, we test the texture discrimination performance with the SVM classifier. Finally, we convey classified texture information to the user using sensory feedback. Our work represents several transformative steps leading to a novel soft biomimetic finger design with a

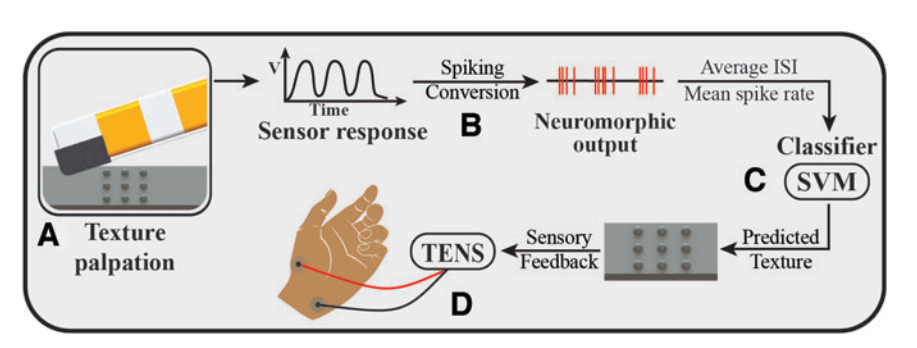


FIG. 1. Overview of the texture discrimination method using the soft biomimetic finger. (A) Texture palpation using the soft finger with the tactile sensor. (B) The sensor response is neuromorphically encoded using the Izhikevich neuron model to mimic SA-1 neuron spiking patterns. (C) The spike-based features, average ISI, and mean spike rate are used as inputs for SVM to classify the textures. (D) Sensory feedback is then provided to the user through TENS. ISI, interspike interval; SA-1, slowly adapting; SVM, support vector machine; TENS, transcutaneous electrical nerve stimulation. Color images are available online.

■F1

SOFT FINGER TEXTURE DISCRIMINATION AND SENSORY FEEDBACK

flexible sensor and capability to palpate textures and subsequently provide sensory feedback.

Design and Fabrication

Sensor array design

Sensors incorporated into soft robots prioritize flexibility and simple fabrication to minimize its effect on the robot's actuation. The design of the flexible, textile tactile sensor F2 array (Fig. 2) was inspired by the mechanoreceptors found in the epidermis of the human body. 48 This variation of a piezoresistive tactile sensor was easily integrated with the fingertip of the soft biomimetic finger, which was fabricated mainly from silicone and fabric. Additionally, the sensor does not interfere with the normal actuation of the soft biomimetic finger. The 3×3 tactile sensor array has nine taxels, or sensing elements, to convey spatial information about the textures. This type of sensor can be easily scaled to cover a larger surface area with more taxels to provide additional spatial information.

The tactile sensor was fabricated using conductive fabric traces (LessEMF, Latham, NY) and piezoresistive fabric (Eonyx, Pinole, CA), which transforms the force applied on

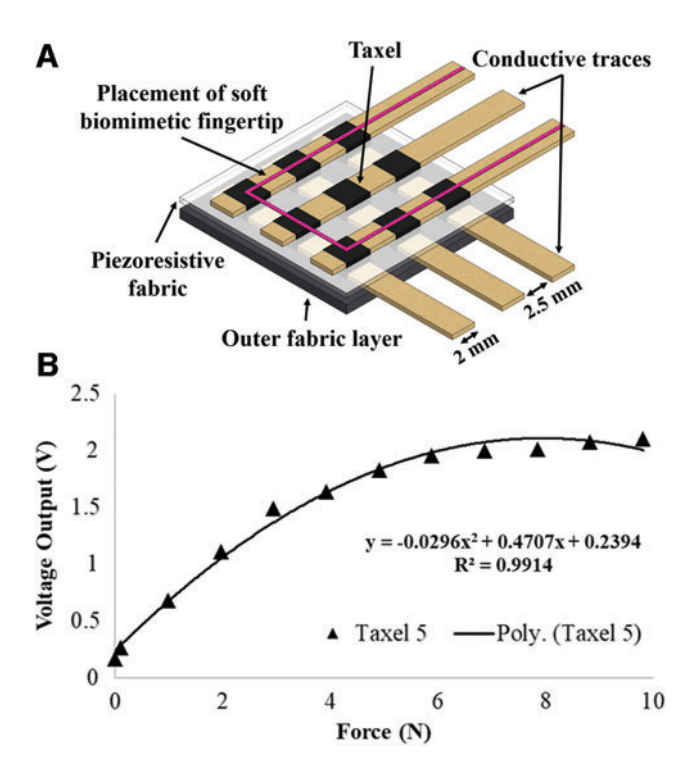


FIG. 2. (A) Graphic of the flexible textile tactile sensor array. The 3×3 sensor array has nine 4 mm^2 taxels (or sensing elements) spaced 2.5 mm apart. The tactile sensor array is integrated at the fingertip of the soft biomimetic finger. (B) The characterization curve of the tactile sensor (Force vs. Voltage response) was created by placing 11 calibration weights, ranging from 10 to 1000 g, onto the taxel using an end-effector tip. Each weight was applied once per taxel. The characterization curve of the center taxel, taxel 5, is shown as it makes the most direct contact with the textures. The other taxels follow a similar curve with a consistent range of linear response. Color images are available online.

the material into changes in resistance. The piezoresistive fabric is sandwiched between 2 mm perpendicular crossing strips of conductive fabric. This creates a $2 \times 2 \,\mathrm{mm}^2$ sensing surface area for each taxel. The conductive fabric traces are spaced 2.5 mm apart. A black, protective, elastic fabric encases the entire sensor array. Due to these low-cost materials, the textile tactile sensor benefits from a low manufacturing cost.

The voltage response of the tactile sensor array was measured using an Arduino Mega 2560 microcontroller. Each common line of the sensor was connected in series with a 10 $k\Omega$ resistor, acting as a voltage divider. For this study, the exact value of the applied force is not necessary, as the texture discrimination method with neuromorphic encoding uses the relative forces measured across the textures.

Soft biomimetic finger design

The pneumatically actuated soft biomimetic finger has three joints with two independently controllable DOF, similar to a human finger (Fig. 3). It was fabricated from Dragon ◀F3 SkinTM 10 Medium (Smooth-on, Macungie, PA) silicone rubber and two inextensible materials, cotton fiber and cotton fabric. 28 The fracture strength for the silicone rubber, which is the measure of the material's ability to resist failure during elongation, is 1000%. Dragon Skin rubbers have previously been used for applications from medical prosthetics to special skin effects. ^{9,49,50} Since the soft biomimetic finger was constructed from silicone and fabric, it has a low manufacturing cost and is very compliant.

Using the concept of hybrid fiber reinforced actuators, 51 the two inextensible materials behave as strain-limiting layers to reinforce the actuator and prevent radial expansion. To create the air channels in the actuator, the silicone prepolymer was poured over carbon fiber rods, separated by a block of silicone, during the fabrication process. The carbon fiber rods serve as the template for the air cavity and the block of silicone separates the two air channels. Next, two layers of cotton fiber (0.1 mm thickness) were wound around the cured

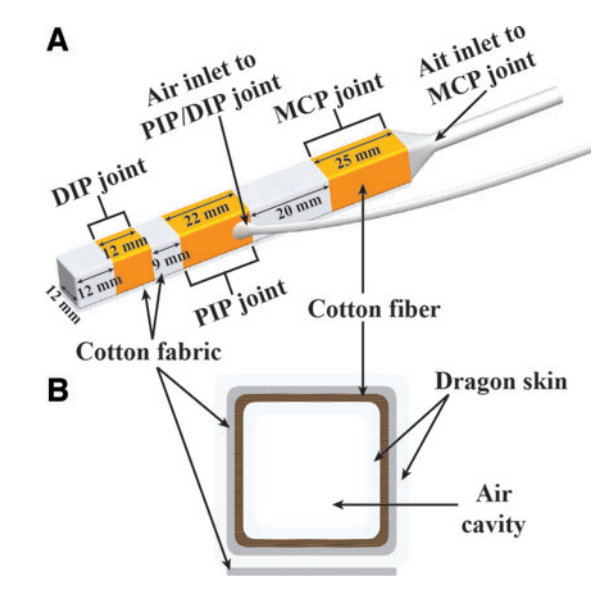


FIG. 3. (A) Isometric view of the soft biomimetic finger model. (B) Graphical cross section of the soft finger. Color images are available online.

silicone inner bladder with a pitch of 0.4 mm to completely cover the inner bladders. Next, three strips of cotton fabric, one 20 mm and two 8 mm width strips, with a length of 96 mm were applied at specific intervals along the soft finger. The 20 mm strip was applied around the section of silicone between the two pneumatic channels to mimic the proximal phalange. The 8 mm strips were applied on the soft biomimetic finger at specific intervals to mimic the distal and intermediate phalanges of a human finger. The sections of silicone not wrapped with these fabric strips are intended to create the metacarpophalangeal (MCP), proximal interphalangeal, and distal interphalangeal joints (Fig. 3). The fiber and fabric-reinforced inner section was then coated with a final layer of silicone. To seal the fingertip, a small silicone rod and silicone glue were added to the distal end of the soft finger. Finally, a strip of fabric, 100 mm by 12 mm, was adhered to the palmar surface of the soft finger. This final strainlimiting layer of fabric creates the directional curvature that mimics the human finger. Through this process, the pneumatically actuated soft biomimetic finger's three joints with two DOF was created.

The angle of flexion of the soft biomimetic finger is determined by the actuation pressure, with a linear relationship during simultaneous actuation of both air channels (Fig. 4). The pneumatic setup (Fig. 4C) used an air compressor and two three-way direct-acting solenoid valves to regulate the air flow into the soft biomimetic finger. Each valve is connected to an air channel's inlet and a pressure sensor (Honeywell ASDXACX100PAAA5). The pneumatic circuit is independently controlled by an Arduino microcontroller.

Textured plates design

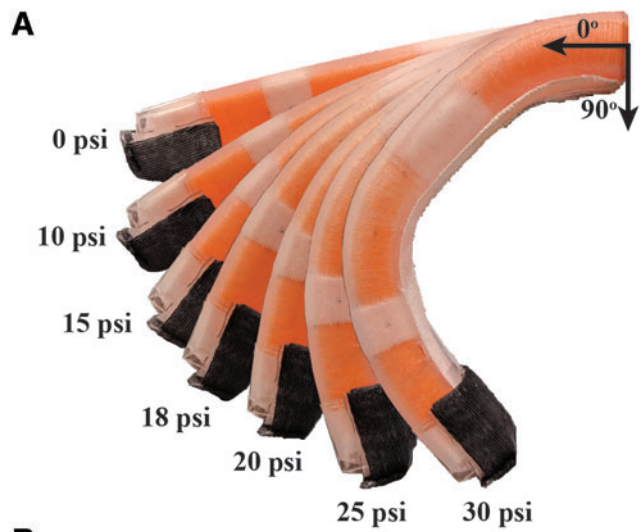
A total of 13 textured plates were designed and 3D printed out of polylactic acid (PLA) to assess the soft finger's texture discrimination capability (Fig. 5). These $108 \times 36 \text{ mm}^2$ textured plates, with varying texture elements, were passively palpated by the soft biomimetic finger. The varied texture elements of the textured plates require both spatial and temporal information to accurately discriminate between the textures. The $36 \times 36 \text{ mm}^2$ textured surface was centered along the plate to create an isolated surface for palpation. Each texture was raised 2.5 mm above the top plane of the textured plate.

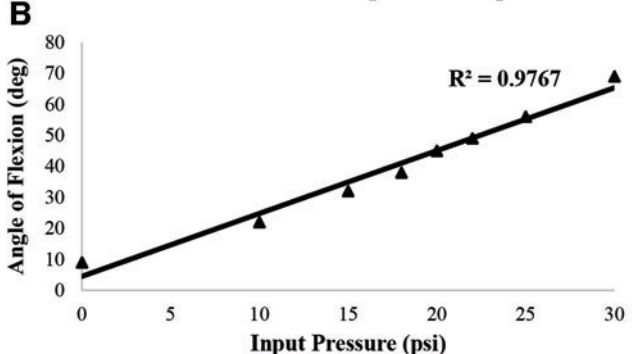
Methods

To test texture discrimination in this study (Fig. 1), the soft finger passively palpated the 13 textured plates at 4 speeds and 4 actuated states. This resulted in 16 total parameters being tested over the 13 textured plates to determine the texture discrimination ability of the soft finger at varying conditions.

Experimental procedure

Consistent palpation of the textures required a robust testing method with a gripper that held the soft biomimetic finger without inhibiting its actuation. Thus, the soft finger's MCP inlet was held by the gripper to allow normal actuation and was mounted to an UR5 Robot arm (Universal Robots, Odense, Denmark) to palpate the textured plates. First, the soft biomimetic finger was brought down onto one side of the textured plate until the fingertip was between 10° and 15° with respect to the textured plate and applied a normal force





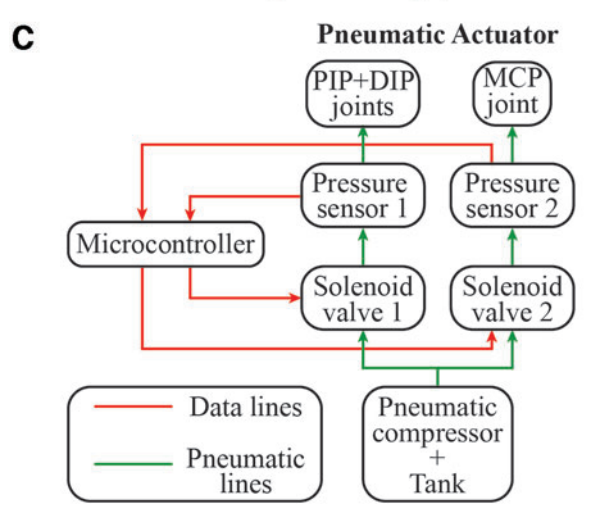


FIG. 4. (**A**) Side view of the simultaneous actuation of both joints at varying pressures when mounted horizontally on the UR5 robot arm. (**B**) Angle of flexion of the soft biomimetic finger in response to the pneumatic actuation pressure. The angle of flexion is the degree to which the fingertip moved when the soft finger flexed during actuation compared with the 0° horizontal reference at the base of the soft finger. (**C**) Overview of the pneumatic setup used to actuate the soft finger. Color images are available online.

of 1 N (Fig. 6). The soft finger was held at this angle to $\P6$ achieve maximum surface contact of the sensor onto the texture. Then, the soft finger palpated the textured plates by being moved along the direction shown in Figure 5. Finally, the soft finger was moved back up and to the start position. A

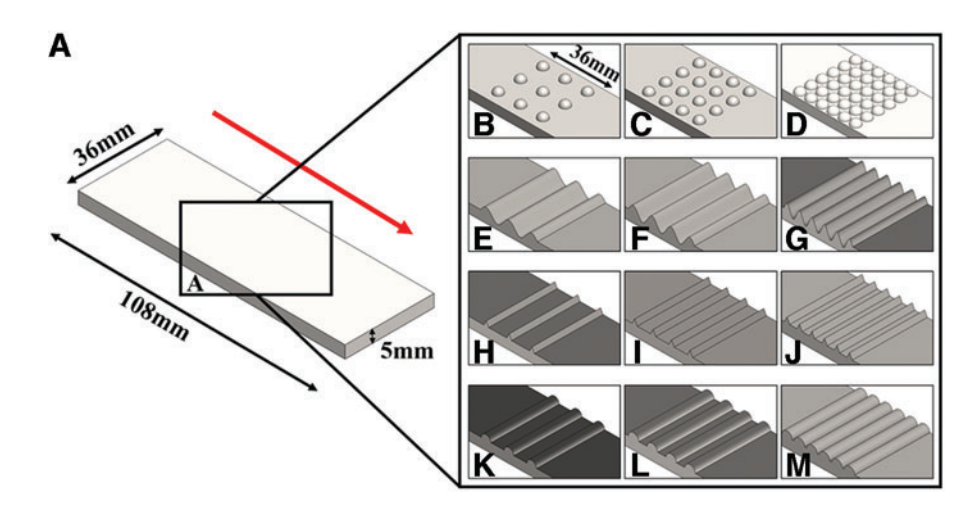


FIG. 5. Textured plates designed to test the soft biomimetic finger's ability to discriminate textures. The four main texture elements are hemispheres (B–D), sinusoidal waves (E–G), triangular ridges (H–J), and curved ridges (K–M). These texture elements were varied by 3, 4, or 6 rows and combined with the flat (A) texture created 13 total textured plates. The red arrow indicates the direction of palpation. Color images are available online.

complete loop of the UR5 robot arm was considered one trial. Each of the 13 textures was palpated with 80 trials for all 16 parameters. The voltage response of each taxel was sampled by the Arduino Mega 2560 microcontroller at 100 Hz and processed in MATLAB.

With the goal of comprehensively testing the texture discrimination capability of the soft biomimetic finger at different conditions, tests occurred at varying speeds of palpation and levels of actuation. To test the ability of the soft finger at varying speeds of palpation, the UR5 robot arm moved the soft finger at 23, 44, 64, and 81 mm/s. The soft finger was also tested at varying pressure levels for simultaneous joint actuation: 0, 10, 15, and 18 psi. This changed the duration of each trial for the 16 parameters, which is shown in Table 1. Although the soft biomimetic finger could actuate up to 30 psi and create a larger bending angle, this was not feasible in this testing environment. Beyond 18 psi, proper contact of the fingertip to the textures on the plates was not achievable.

Neuromorphic encoding

Neuromorphic encoding was used due to its computational efficiency in encoding information and its biological relevance for afferent nerve stimulation.^{33,52,53} The encoding of spatial and temporal information is important when processing dynamic cues such as texture. The Izhikevich neuron model was used to mimic the mechanoreceptor activity of the tactile epithelial cells called Merkel cells.⁵⁴ To utilize the

Izhikevich framework, the tactile response from each taxel was converted using the tonic spiking model. This model exhibits a steady-state spiking pattern after the initial onset and is used as the basis for the slowly adapting (SA-1) neuron spiking patterns (Fig. 7). This neuromorphic encoding method has been used previously for similar applications. Probable 19,33,44,46 The Izhikevich neuron model uses Equations (1)–(3) to generate the spike train with injected current I, neuronal membrane voltage v, and recovery variable u, which represents the activation and inactivation of K^+ and Na^+ ionic channels.

$$\frac{dv}{dt} = 0.04v^2 + 5v + 140 - u + kI \tag{1}$$

$$\frac{du}{dt} = a(bv - u) \tag{2}$$

if
$$v \ge 30 \text{ mv}$$
, then $\begin{cases} v \leftarrow c \\ u \leftarrow u + d \end{cases}$ (3)

The voltage response of each taxel was normalized and a gain factor, k, of 75 was applied, which was best for classification. This normalized and amplified signal served as the input current for the neuron spiking model. The Tonic Spiking model's parameters are a = 0.02, b = 0.2, c = -65, and d = 8.

For each texture and testing parameter, the spiking responses from the sensor array were segmented into windows

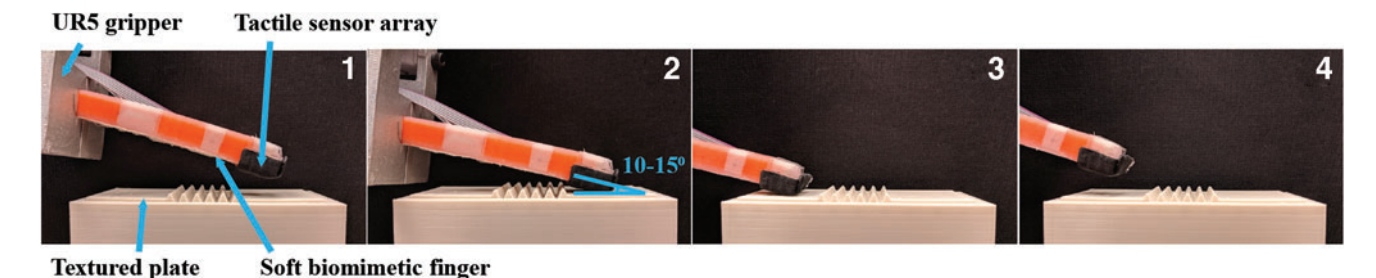


FIG. 6. Overview of the different positions of the soft biomimetic finger in a trial with the positions numbered in chronological order. The soft finger was mounted on the UR5 robot arm and is shown during passive palpation of textured plate G, while at 0 psi. The soft finger was held at 10–15° compared with the textured plate. In position (2), the soft biomimetic finger is brought down until it applies 1 N of force, measured on taxel 5. Color images are available online.

Table 1.	DURATION	OF A	SINGLE	Trial
1	FOR EACH F	ARAN	TETER	

Durations (s)	Palpation speed (mm/s)				
	23	44	64	81	
Actuated pressu	re (psi)				
0	9.8 s	5.65 s	4.27 s	$3.57 \mathrm{s}$	
10	10.62 s	$6.06 \mathrm{s}$	4.54 s	$3.78 \mathrm{s}$	
15	11.54 s	$6.52 \mathrm{s}$	4.84 s	$4.01 \mathrm{s}$	
18	12.15 s	$6.82\mathrm{s}$	5.05 s	4.16 s	

corresponding to the duration of the loop based on each parameter (Table 1). These windows were converted offline into spike trains with the Izhikevich neuromorphic model. To compress the information and serve as the features for the classification algorithm, the average interspike interval and mean spike rate were calculated for each taxel in every trial window. The average interspike interval was calculated by measuring the time elapsed between spikes and averaging those values in each window. The mean spike rate was calculated by tallying the number of spikes in 100 ms bins and dividing it by the bin length, followed by averaging those values in each window.

Classification algorithms

To test the ability of the soft biomimetic finger to classify textures, the two features from each taxel in a window were used as inputs for SVMs multiclass linear classification model. Specifically, the linear kernel of SVM from MA-TLAB was used because the assumptions of normal distribution and similar within-class variance were not required. A supervised learning algorithm was chosen because the identities of the textures were known. In our preliminary texture discrimination studies, this classification algorithm has been shown to classify textures well. 29,46

Eighteen features, two per taxel for each trial, from the compressed spiking information were used as the input for the classifier. To reduce the bias of the model, the k-fold cross-validation procedure was performed using the classical statistical methods. 55,56 This procedure randomly splits the data set into k groups. Then, a single group is taken out as the test data set and the remaining groups are used as the training data set. A model is first fit on the training data set and subsequently evaluated on the test data set. Finally, the evaluation score is retained and the same process is completed on the remaining groups. The final classification accuracy is the combination of the result from all groups. In this experiment,

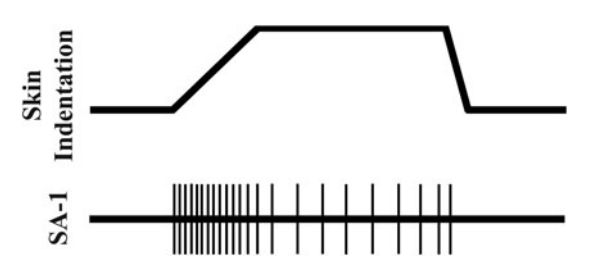


FIG. 7. Spiking response of an SA-1 neuron in response to a tactile stimulus.

a k=4 was used on the 80 trials per texture plate, resulting in splits of 75% training and 25% testing.

Sensory feedback

Upon classification of the textures, the textural information should then be conveyed to the user. To investigate whether a user would be able to differentiate different textures, transcutaneous electrical nerve stimulation (TENS) was used for sensory stimulation. This technique has been used previously for conveying touch and pressure information to an amputee. 44,57 As a demonstration of sensory feedback for textures, four stimulation conditions based on frequency and pulse width were tested. These four stimulation conditions represented a subset of four textures with varied textural information but did not directly correspond to those texture patterns. Three healthy able-bodied subjects participated in this study that was approved by the Johns Hopkins Medicine Institutional Review Board. Sensory mapping was first performed to obtain a stimulation site on the subject's wrist that activated referred sensation in their hand. During sensory mapping, a beryllium copper (BeCu) probe was connected to the isolated current stimulator (DS3; Digitimer Ltd.), which provided a monophasic current. A 5 mm disposable Ag/AgCl electrode (Norotrode 20; Myotronics) was placed on the stimulation site for three psychophysical experiments.

To determine the stimulation frequency that separates discrete and continuous perception of sensation at the referred sensation site in the phantom hand, a discrete vs. continuous frequency detection experiment was conducted.⁵⁷ Two frequencies from this experiment were selected and designated as the low-frequency (discrete) and high-frequency (continuous) conditions. Then, to determine the minimum level of stimulation that is detectable by the subject, a stimulation detection experiment was subsequently conducted.⁵⁷ The pulse width of the stimulation was varied while the frequency was held constant at the previous discrete or continuous frequency value. From this experiment, two pulse widths were selected and designated as the low-intensity and high-intensity conditions. For each experiment, the subject received 2 s of stimulation and verbally indicated if they perceived the stimulation as discrete or continuous. The data were fitted with a psychometric function using a sigmoid as shown in Equation (4), where α is the detection threshold and β is the discrimination sensitivity.

$$\frac{1}{1 + e^{-(x - \alpha)/\beta}}\tag{4}$$

Finally, a conditional discrimination experiment was conducted to investigate whether the subjects could differentiate one condition from another. The subjects were presented with two 2-s stimulations, with a 1-s interval. The subjects then reported whether they perceived the two stimulations as the same or different. Table 2 shows the pulse width and fre- ◀T2 quency parameters used for the condition discrimination experiment for each subject (AB01, AB02, and AB03).

Results and Discussion

Neuromorphic encoding

The voltage response from the tactile sensor was converted into spiking patterns by passing it through the neuromorphic

SOFT FINGER TEXTURE DISCRIMINATION AND SENSORY FEEDBACK

Table 2. Stimulation Parameters for the Condition Discrimination Experiment

	Subject					
	AB01		AB02		AB03	
Condition	PW (ms)	Frequency (Hz)	PW (ms)	Frequency (Hz)	PW (ms)	Frequency (Hz)
1	1	10	2.5	10	5	5
2 3	10 1	10 50	10 2.5	10 50	10 5	5 50
4	10	50	10	50	10	50

PW, pulse width.

F8 model (Fig. 8). SA-1 neurons primarily respond to the amplitude of the injected current. Therefore, they spike throughout the presence of a texture, following the spatial features of that texture. As such, the spike train generated through passive palpation followed the spatial features of the textures. Due to the compliance of the soft biomimetic finger and flexible tactile

> **Texture B Texture E** Normalized Voltage Potential (mV) Time (s) Time (s) **Texture H Texture K**

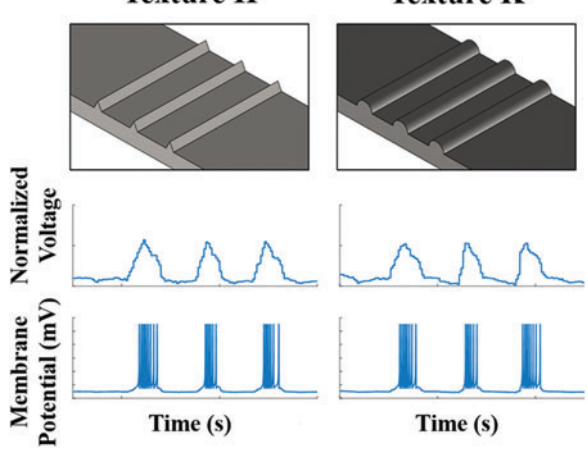


FIG. 8. Spiking responses from a single taxel on the tactile sensor based on the voltage responses from Textures B, E, H, and K. The spiking responses shown were from the soft biomimetic finger when it palpated the textures at 23 mm/s and was actuated to 15 psi. Color images are available online.

sensor, the spatial features of the textured plates were accentuated and provided a distinct and reliable response to each texture.

Classification performance

The soft biomimetic finger was tested at four speeds of palpation and four levels of actuation. The goal was to test the soft biomimetic finger over the 16 parameters to characterize and show how accurately it was able to classify the textures. When run through the pipeline, the soft finger was able to reliably classify all 13 textures at each of the parameters. The overall classification accuracies of each parameter are shown in Table 3. The average of the overall classification accura- ◀T3 cies for the parameters was 99.57%.

The confusion matrix of one parameter, 23 mm/s and 15 psi actuation, is shown in Figure 9. Concurring with the overall ◀F9 accuracy of 99.62% of this parameter, the class accuracies do not drop less than 93.66%, with Texture G (six Sinusoidal waves) being the only one that caused some confusion for the SVM classifier. The soft biomimetic finger benefits from its pliancy and the spatial integration of the taxels in the flexible tactile sensor array when discriminating textures. These results confirm the robust and high-performing texture discrimination capability of the neuromorphic encoding algorithm. Next, we demonstrate the resultant sensory feedback to the user.

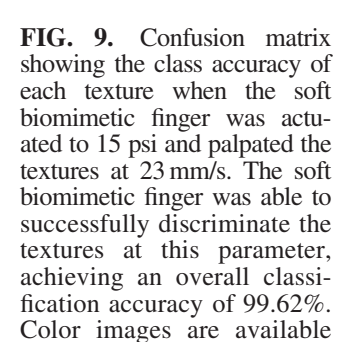
Sensory feedback

Three able-bodied subjects participated in the stimulation psychophysical experiments. The results of the conditional discrimination experiment are shown in Figure 10, where the ◀F10 rows represent the condition presented first and the columns represent the condition presented second. Subjects AB01 and AB02 were able to differentiate between three conditions, whereas subject AB03 was able to differentiate between two conditions. The ability to discriminate between stimulation

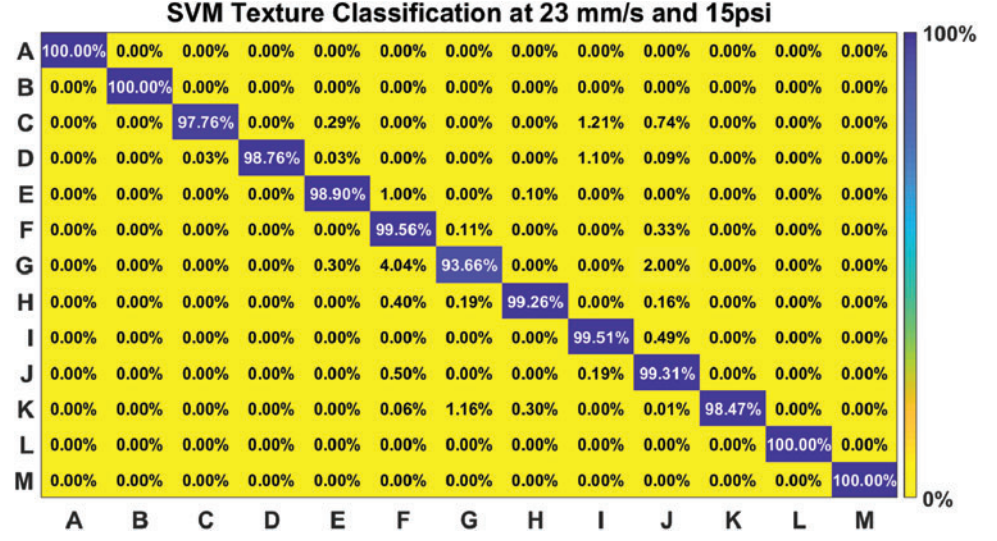
TABLE 3. THE OVERALL CLASSIFICATION ACCURACIES OF THE SOFT BIOMIMETIC FINGER IN EACH PARAMETER

Actuated pressure (psi)		s)		
	23	44	64	81
0	98.65%	99.52%	99.90%	99.52%
10	99.33%	99.62%	99.04%	99.81%
15	99.62%	99.42%	99.42%	99.81%
18	99.71%	100.00%	99.71%	100.00%

8 SANKAR ET AL.



online.



frequencies or intensities varied among subjects. Subject AB01 had difficulty in separating discrete versus continuous pattern at low stimulation intensity (Fig. 10A). Subject AB02 had difficulty in separating low versus high intensity for the continuous stimulation pattern (Fig. 10B). Subject AB03, however, could only determine difference in discrete vs. continuous patterns, but not intensity (Fig. 10C).

Rigid finger comparison

The texture discrimination experiment was also run using the same tactile sensor array attached to the fingertip of the index finger on a Touch Bionics prosthetic hand. This was performed to compare how well the soft finger was able to classify soft and hard textures compared with a rigid finger. For this comparison, another set of textured plates, identical to those shown in Figure 5, were fabricated out of Dragon Skin 10 silicone, referred to as soft textured plates. The soft biomimetic finger and rigid prosthetic finger passively palpated these soft textured plates and the original hard textured plates, with 40 trials for each of the 26 textures.

Overall, the soft finger performed on par with the rigid finger, with a slight improvement at discriminating the soft textures. The soft finger achieved an accuracy of 98.65% for both soft and hard textures, whereas the rigid finger obtained

an accuracy of 98.27% for hard textures and 97.31% for soft textures. Although the differences are small, the drop in performance of soft texture discrimination for the hard finger could indicate the benefit of the soft finger to discriminate soft textures.

Discussion

A soft finger with a soft compliant sensor and neuromorphic encoding attempts to mimic a human finger. Our study finds that this combination of features has many attributes of human fingers. The compliance of the soft finger would aid it in palpating softer materials. However, further exploration is needed to determine the relative benefits of our soft finger solution compared with the current hard finger design as the results from our limited study of textures between the two were comparable. Additionally, our study did not include objects of different curvatures. Still, the benefits of the soft finger, such as suitability to handle delicate objects, could pave the way for a hybrid biomimetic or andromorphic finger solution, combining the advantages of both soft and hard materials.

Sensors incorporated into soft robots prioritize flexibility and simple fabrication to minimize its effect on the robot's actuation. Therefore, the primary design constraint of our sensor is that it

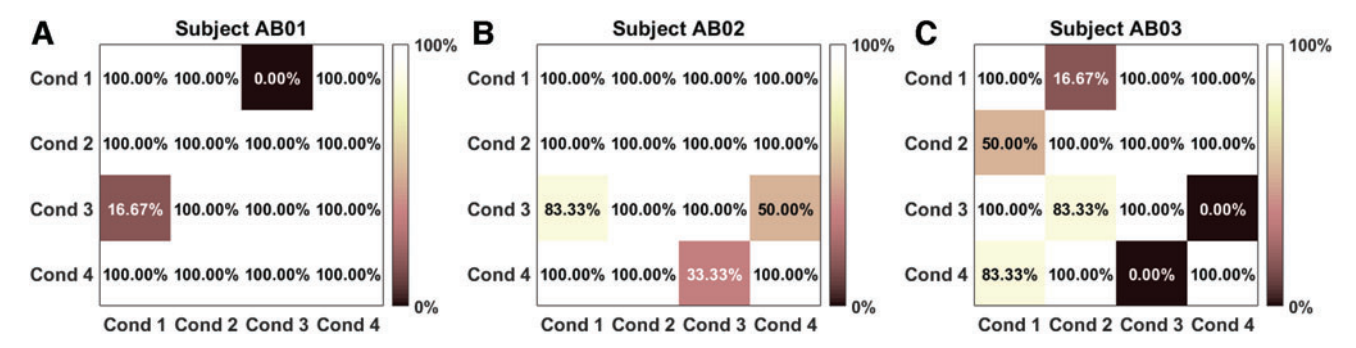


FIG. 10. Condition discrimination results for subjects AB01 (A), AB02 (B), and AB03 (C). Each grid shows the percentage at which the subject was able to identify if the conditions presented were the same or different. Color images are available online.

SOFT FINGER TEXTURE DISCRIMINATION AND SENSORY FEEDBACK

needs to be flexible and cannot interfere with the normal actuation of the soft biomimetic finger. Based on this, we created a novel flexible, textile tactile sensor for the soft biomimetic finger, with neuromorphic output that performed well at texture discrimination.

With the current selection of textures, the soft finger was able to classify the textures with a high level of accuracy. A texture database, which includes finer natural textures, would help validate and test this method further.³⁷ Decoding algorithms such as Victor-Purpura distance and van Rossum distance with spiking neural networks can also provide more information about the textures and improve classification performance. 30,37 Additionally, the design of the flexible tactile sensor array with overlapping receptor fields allows the use of super resolution. By involving spatial averages over the taxels in the sensor array, the ability to sense at a higher acuity is possible. This is a technique used to enhance the resolution of an imaging system.⁵⁸ The human body is also able to perceive textures regardless of the speed of palpation. This speed invariance could be achieved using a modified neuromorphic model and testing with a similar method. Finally, by using multiple soft biomimetic fingers in unison, grasping and manipulating objects with texture recognition while providing sensory feedback is

Since the subjects were only able to differentiate between a few conditions, static stimulation using TENS may not be enough to convey all the current textural information. However, dynamic stimulation of the user with the neuromorphic output could convey more information. Using these sensory feedback methods, a more natural perception of the environment can occur and ultimately aid in prosthetic embodiment. Additionally, this work will be useful in human–machine interactions, such as co-robotics, especially as robotic hands and human hands interact.

Conclusion

Our study demonstrates the ability of the soft biomimetic finger to accurately differentiate textures with the added potential to provide users the ability to perceive their environment while interacting with it. The andromorphic nature of the soft biomimetic finger, with its softness, compliance, and neuromorphic mechanoreceptor-like spiking responses, makes it best suited to bring robotic and prosthetic technology closer to a natural finger.

Furthermore, we showed that a novel soft, three-jointed biomimetic finger with two DOF and the ability to discriminate textures using a flexible textile tactile sensor array can palpate textures and then convey classified texture information to the user using sensory feedback. At different independent speeds of palpation and levels of actuation parameters, the soft biomimetic finger was able to classify textures with very high accuracy. Thus, our work demonstrates the soft finger with biomimetic tactile sensors and neuromorphic encoding can be used for palpation applications, especially texture discrimination tasks.

Acknowledgments

The authors express their gratitude to the two anonymous reviewers for their constructive comments and suggestions on the earlier draft of the article.

Author Disclosure Statement

All authors declare no competing financial interests.

Funding Information

■AU4

This research was funded by a grant from the Office of Naval Research (Global) to the Singapore Institute of Neurotechnology and the NSF award 1830444 under the National Robotics Initiative to Johns Hopkins University.

References

- Sornkarn N, Nanayakkara T. Can a soft robotic probe use stiffness control like a human finger to improve efficacy of haptic perception? IEEE Trans Haptics 2017;10:183– 195.
- Abidi H, Gerboni G, Brancadoro M, et al. Highly dexterous 2-module soft robot for intra-organ navigation in minimally invasive surgery. Int J Med Robotics Comput Assist Surg 2018;14:e1875.
- 3. Diodato A, Brancadoro M, De Rossi G, *et al.* Soft robotic manipulator for improving dexterity in minimally invasive surgery. Surg Innov 2018;25:69–76.
- Shiva A, Stilli A, Noh Y, et al. Tendon-based stiffening for a pneumatically actuated soft manipulator. IEEE Robot Autom Lett 2016;1:632–637.
- 5. Polygerinos P, Wang Z, Galloway KC, *et al.* Soft robotic glove for combined assistance and at-home rehabilitation. Robot Auton Syst 2015;73:135–143.
- 6. Park Y-L, Chen B, Pérez-Arancibia NO, *et al.* Design and control of a bio-inspired soft wearable robotic device for ankle–foot rehabilitation. Bioinspir Biomim 2014;9: 016007.
- 7. Huaroto JJ, Suarez E, Krebs HI, *et al.* A soft pneumatic actuator as a haptic wearable device for upper limb amputees: Toward a soft robotic liner. IEEE Robot Autom Lett 2019;4:17–24.
- 8. Thompson-Bean E, Das R, McDaid A. Methodology for designing and manufacturing complex biologically inspired soft robotic fluidic actuators: prosthetic hand case study. Bioinspir Biomim 2016;11:066005.
- Yap HK, Khin PM, Koh TH, et al. A fully fabric-based bidirectional soft robotic glove for assistance and rehabilitation of hand impaired patients. IEEE Robot Autom Lett 2017;2:1383–1390.
- Rocha RP, Lopes PA, de Almeida AT, et al. Fabrication and characterization of bending and pressure sensors for a soft prosthetic hand. J Micromech Microeng 2018;28: 034001.
- Shahid Z, Glatman AL, Ryu SC. Design of a soft composite finger with adjustable joint stiffness. Soft Robot 2019;6: 722-732.
- Deimel R, Brock O. A novel type of compliant and underactuated robotic hand for dexterous grasping. Int J Robot Res 2016;35:161–185.
- Zhao H, O'Brien K, Li S, et al. Optoelectronically innervated soft prosthetic hand via stretchable optical waveguides. Sci Robot 2016;1:eaai7529.
- Feng N, Shi Q, Wang H, et al. A soft robotic hand: Design, analysis, SEMG control, and experiment. Int J Adv Manuf Technol 2018;97:319–333.
- Devi MA, Udupa G, Sreedharan P. A novel underactuated multi-fingered soft robotic hand for prosthetic application. Robot Auton Syst 2018;100:267–277.

10 SANKAR ET AL.

 Feng N, Wang H, Hu F, et al. A fiber-reinforced humanlike soft robotic manipulator based on SEMG force estimation. Eng Appl Artif Intell 2019;86:56–67.

- Liang Z, Cheng J, Zhao Q, et al. High-performance flexible tactile sensor enabling intelligent haptic perception for a soft prosthetic hand. Adv Mater Technol 2019;4: 1900317.
- Fras J, Althoefer K. Soft biomimetic prosthetic hand: Design, manufacturing and preliminary examination. In 2018 IEEE/RSJ International Conference on Intelligent Robots and Systems (IROS); IEEE, Madrid, 2018, pp. 1–6.
- Suzumori K, Maeda T, Wantabe H, et al. Fiberless flexible microactuator designed by finite-element method. IEEE/ ASME Trans Mechatron 1997;2:281–286.
- Trivedi D, Rahn CD, Kier WM, et al. Soft robotics: Biological inspiration, state of the art, and future research. Appl Bionics Biomech 2008;5:99–117.
- 21. Lee C, Kim M, Kim YJ, et al. Soft robot review. Int J Control Autom Syst 2017;15:3–15.
- Truby RL, Wehner M, Grosskopf AK, et al. Soft somatosensitive actuators via embedded 3D printing. Adv Mater 2018;30:1706383.
- Low JH, Lee WW, Khin PM, et al. Hybrid tele-manipulation system using a sensorized 3-D-printed soft robotic gripper and a soft fabric-based haptic glove. IEEE Robot Autom Lett 2017;2:880–887.
- Bholat OS, Haluck RS, Kutz RH, et al. Defining the role of haptic feedback in minimally invasive surgery. Stud Health Technol Inform 1999;62:62–66.
- Ong R, Glisson CL, Burgner-Kahrs J, et al. A novel method for texture-mapping conoscopic surfaces for minimally invasive image-guided kidney surgery. Int J CARS 2016; 11:1515–1526.
- Johansson RS, Flanagan JR. Coding and use of tactile signals from the fingertips in object manipulation tasks. Nat Rev Neurosci 2009;10:345–359.
- 27. Su Z, Fishel JA, Yamamoto T, *et al.* Use of tactile feedback to control exploratory movements to characterize object compliance. Front Neurorobot 2012;6:7.
- Balamurugan D, Nakagawa-Silva A, Nguyen H, et al. Texture discrimination using a soft biomimetic finger for prosthetic applications. In 2019 IEEE 16th International Conference on Rehabilitation Robotics (ICORR); IEEE, Toronto, ON, Canada, 2019, pp. 380–385.
- Sankar S, Brown A, Balamurugan D, et al. Texture discrimination using a flexible tactile sensor array on a soft biomimetic finger. In 2019 IEEE SENSORS; IEEE, Montreal, QC, Canada, 2019, pp. 1–4.
- AU5 30. Yi Z, Zhang Y. Recognizing tactile surface roughness with a biomimetic fingertip: A soft neuromorphic approach. Neurocomputing 2017;244.
- AU6 ► 31. Qin L, Zhang Y. Roughness discrimination with bio-inspired tactile sensor manually sliding on polished surfaces. Sensor Actuat A Phys 2018;279.
- AU7 ▶ 32. Qin L, Yi Z, Zhang Y. Enhanced surface roughness discrimination with optimized features from bio-inspired tactile sensor. Sensor Actuat A Phys 2017;264.
 - Rasouli M, Chen Y, Basu A, et al. An extreme learning machine-based neuromorphic tactile sensing system for texture recognition. IEEE Trans Biomed Circuits Syst 2018; 12:313–325.
 - 34. Kim S-H, Engel J, Liu C, *et al.* Texture classification using a polymer-based MEMS tactile sensor. J Micromech Microeng 2005;15:912–920.

- 35. Chun S, Kim Y, Oh H-S, *et al.* A highly sensitive pressure sensor using a double-layered graphene structure for tactile sensing. Nanoscale 2015;7:11652–11659.
- 36. Chun S, Hong A, Choi Y, *et al.* A tactile sensor using a conductive graphene-sponge composite. Nanoscale 2016;8: 9185–9192.
- Rongala UB, Mazzoni A, Oddo CM. Neuromorphic artificial touch for categorization of naturalistic textures. IEEE Trans Neural Netw Learning Syst 2017;28:819–829.
- 38. Cao Y, Li T, Gu Y, *et al.* Fingerprint-inspired flexible tactile sensor for accurately discerning surface texture. Small 2018;14:e1703902.
- 39. Song A, Han Y, Hu H, *et al.* A novel texture sensor for fabric texture measurement and classification. IEEE Trans Instrum Meas 2014;63:1739–1747.
- Jamali N, Sammut C. Majority voting: Material classification by tactile sensing using surface texture. IEEE Trans Robot 2011;27:508–521.
- 41. Muhammad HB, Recchiuto C, Oddo CM, *et al.* A capacitive tactile sensor array for surface texture discrimination. Microelectron Eng 2011;88:1811–1813.
- 42. Gupta AK, Ghosh R, Swaminathan AN, et al. A neuro-morphic approach to tactile texture recognition. In 2018 IEEE International Conference on Robotics and Biomimetics (ROBIO); IEEE, Kuala Lumpur, Malaysia, 2018, pp. 1322–1328.
- Mazzoni A, Rongala UB, Oddo CM. Decoding of naturalistic textures from spike patterns of neuromorphic artificial mechanoreceptors. BMC Neurosci 2015;16(Suppl 1): P186.
- 44. Osborn LE, Dragomir A, Betthauser JL, *et al.* Prosthesis with neuromorphic multilayered e-dermis perceives touch and pain. Sci Robot 2018;3:eaat3818.
- 45. Raspopovic S, Capogrosso M, Petrini FM, *et al.* Restoring natural sensory feedback in real-time bidirectional hand prostheses. Sci Transl Med 2014;6:222ra19.
- 46. Nguyen H, Osborn L, Iskarous M, *et al.* Dynamic texture decoding using a neuromorphic multilayer tactile sensor. In 2018 IEEE Biomedical Circuits and Systems Conference (BioCAS); IEEE, Cleveland, OH, 2018, pp. 1–4.
- 47. Iskarous MM, Nguyen HH, Osborn LE, *et al.* Unsupervised learning and adaptive classification of neuromorphic tactile encoding of textures. In 2018 IEEE Biomedical Circuits and Systems Conference (BioCAS); IEEE, Cleveland, OH, 2018, pp. 1–4.
- 48. Osborn L, Nguyen H, Betthauser J, et al. Biologically inspired multi-layered synthetic skin for tactile feedback in prosthetic limbs. In 2016 38th Annual International Conference of the IEEE Engineering in Medicine and Biology Society (EMBC); IEEE, Orlando, FL, 2016, pp. 4622–4625.
- 49. Yap HK, Goh JCH, Yeow RCH. Design and characterization of soft actuator for hand rehabilitation application (6th European Conference of the International Federation for Medical and Biological Engineering) Lacković I, Vasic D. (Eds). IFMBE Proceedings; Cham: Springer International Publishing, 2015, Vol. 45, pp. 367–370.
- 50. Mazza P, Shin M, Santamaria A. Shape memory alloy ◀AU8 as artificial muscles for facial prosthesis. (Volume 3: Biomedical and Biotechnology Engineering) Tampa, FL: American Society of Mechanical Engineers, 2017, p. V003T04A077.
- 51. Sun Y, Yap HK, Liang X, *et al.* Stiffness customization and patterning for property modulation of silicone-based soft pneumatic actuators. Soft Robot 2017;4:251–260.

- 52. Pearson MJ, Pipe AG, Mitchinson B, *et al.* Implementing spiking neural networks for real-time signal-processing and control applications: A model-validated FPGA approach. IEEE Trans Neural Netw 2007;18:1472–1487.
- 53. Liu S-C, Delbruck T. Neuromorphic sensory systems. Curr Opin Neurobiol 2010;20:288–295.
- 54. Izhikevich EM. Simple model of spiking neurons. IEEE Trans Neural Netw 2003;14:1569–1572.
- Kuhn M, Johnson K. Applied Predictive Modeling. New York: Springer, 2013.
- 56. James G, Witten D, Hastie T, *et al.* An Introduction to Statistical Learning: With Applications in R; Springer texts in statistics. New York: Springer, 2013.
- 57. Osborn L, Fifer M, Moran C, et al. Targeted transcutaneous electrical nerve stimulation for phantom limb sensory feed-

- back. In 2017 IEEE Biomedical Circuits and Systems Conference (BioCAS); IEEE, Torino, 2017, pp. 1–4.
- 58. Hunt BR. Super-resolution of images: algorithms, principles, performance. Int J Imaging SystTechnol 1995;6:297–304.

Address correspondence to: ◀AU9

Sriramana Sankar

Department of Biomedical Engineering

Johns Hopkins University

Baltimore, MD

USA

E-mail: ssankar6@jhu.edu

11

AUTHOR QUERY FOR SORO-2020-0016-VER9-SANKAR_1P

- AU1: Please identify (highlight or circle) all authors' surnames for accurate indexing citations.
- AU2: Please confirm the authors' affiliations and also mention the department name for affiliations 2, 3, and 5.
- AU3: Please include the Clinical Trial Registration number, if applicable, at the end of the abstract.
- AU4: Please confirm the accuracy of the Funding Information. Also include the full name (no abbreviations) of funding agency(ies)/institution(s) and grant numbers.
- AU5: Please mention the page range for "Ref. 30."
- AU6: Please mention the page range for "Ref. 31."
- AU7: Please mention the page range for "Ref. 32."
- AU8: Please mention the editor(s) names for "Ref. 50."
- AU9: Please confirm the address of correspondence. Also please provide the complete address with postal code for the corresponding author's address.